

# The Dimension Six Triple Gluon Operator in Higgs+Jet Observables

Diptimoy Ghosh<sup>1,\*</sup> and Martin Wiebusch<sup>2,†</sup>

<sup>1</sup>*INFN, Sezione di Roma, Piazzale A. Moro 2, I-00185 Roma, Italy*

<sup>2</sup>*Institute for Particle Physics Phenomenology, Department of Physics,  
Durham University, Durham CH1 3LE, United Kingdom*

Recently a lot of progress has been made towards a full classification of new physics effects in Higgs observables by means of effective dimension six operators. Specifically, Higgs production in association with a high transverse momentum jet has been suggested as a way to discriminate between operators that modify the Higgs-top coupling ( $O_t$ ) and operators that induce an effective Higgs-gluon coupling ( $O_g$ )—a distinction that is hard to achieve with signal strength measurements alone. With this article we would like to draw attention to another source of new physics in Higgs+jet observables: the triple gluon operator  $O_{3g}$  (consisting of three factors of the gluon field strength tensor). We compute the distortions of kinematic distributions in Higgs+jet production at a 14 TeV LHC due to  $O_{3g}$  and compare them with the distortions due to  $O_t$  and  $O_g$ . We find that the transverse momentum distributions alone can not discriminate between  $O_{3g}$  and  $O_g$  if the coefficient of the operator  $O_t$  treated as an unknown parameter. We further show that the jet rapidity and the difference between the Higgs and jet rapidity are well suited to remove this new degeneracy. Using rough estimates for the expected bounds we find that allowed distortions in kinematic distributions due to  $O_g$  are of similar size as those due to  $O_{3g}$ . We conclude that a full analysis of new physics in Higgs+jet observables must take the contributions from  $O_{3g}$  into account.

PACS numbers: 12.60.Fr, 12.38.Bx, 14.80.Bn

## I. INTRODUCTION

The discovery of a Higgs resonance whose properties match those of the Standard Model (SM) Higgs boson and the absence of any clear signs of physics beyond the SM in other collider searches suggests that, contrary to many people's expectations, the SM remains valid at energy scales significantly larger than the electroweak scale. In such a situation the language of effective field theory allows us to systematically classify all possible effects that new physics can have on low energy observables in terms of higher dimensional operators. Recently a lot of effort has been dedicated to defining a complete basis of dimension six operators [1–4] and analysing experimental constraints on these operators [5–13].

Determining the Wilson coefficients of all 59 independent dimension six operators clearly requires a large number of experimental observables. Specifically, using only Higgs signal strength measurements as provided by the ATLAS and CMS collaborations [14, 15], it is very difficult to discriminate between the operator  $O_t$  that modifies the  $Ht\bar{t}$  coupling and the operator  $O_g$  that generates an effective  $Hgg$  coupling. (The  $Ht\bar{t}$  coupling is only probed directly in Higgs production in association with a  $t\bar{t}$  pair, and this process is difficult to measure due to its small rate and complicated final state.) As discussed in [16–20] the degeneracy can be broken by measuring kinematic distributions in Higgs production in association with a high  $p_T$  jet. Further studies of kinematic distributions in Higgs+jet production in the presence of

dimension six operators were performed in [21–23] and higher order corrections were considered in [24, 25].

All the above-mentioned studies concentrate on dimension six operators that contain the SM Higgs doublet. With this article we would like to raise awareness for the fact that Higgs production in association with a jet also receives contributions from the triple gluon operator  $O_{3g}$  (consisting of three factors of the gluon field strength tensor). Following the classification of [7] this operator is “loop suppressed” compared to the operators involving the SM Higgs doublet. However, a truly model independent analysis of new physics effects in Higgs+jet production should take these contributions into account. At the very least the Wilson coefficient  $C_{3g}$  of  $O_{3g}$  should appear as a nuisance parameter in the extraction of the Wilson coefficients of other operators from Higgs+jet observables. Constraints from top pair production on  $C_{3g}$  were discussed in [26]. Experimental results for boosted top-pair production from the 7 and 8 TeV LHC runs are presented in [27] but not interpreted in the context of dimension six operators. Here we study the modifications of kinematic distributions in Higgs+jet production due to the triple gluon operator and compare them with those induced by operators involving the Higgs doublet. We find that  $p_T$  distributions alone are insufficient to disentangle the contributions from  $O_t$ ,  $O_g$  and  $O_{3g}$ , and that this degeneracy can be broken by considering rapidity distributions. In particular the rapidity distribution of the extra jet—although incapable of discriminating between modified  $Ht\bar{t}$  and effective  $Hgg$  couplings—turns out to be sensitive to contributions from  $O_{3g}$ .

The presented results are intended as a motivation for more detailed analyses. Hence all our calculations are done at leading order and we do not include parton

\* diptimoy.ghosh@roma1.infn.it

† martin.wiebusch@durham.ac.uk

shower or detector effects. We also postpone the estimation of the experimental sensitivity to the Wilson coefficients to a future publication. Note that, since we are only interested in the shapes of kinematic distributions the inclusion of universal QCD  $K$ -factors is unnecessary for this paper and a fully differential next-to-leading order calculation is clearly beyond its scope.

## II. EFFECTIVE OPERATORS IN $gg \rightarrow Hg$

We consider the effective dimension six Lagrangian

$$\mathcal{L}_6 = \frac{C_g}{\Lambda^2} O_g + \frac{C_{3g}}{\Lambda^2} O_{3g} + \left( \frac{C_t}{\Lambda^2} O_t + \text{h.c.} \right) + \left( \frac{C_b}{\Lambda^2} O_b + \text{h.c.} \right), \quad (1)$$

where  $\Lambda$  is the scale of new physics,  $C_g$ ,  $C_{3g}$ ,  $C_t$ , and  $C_b$  are dimensionless Wilson coefficients and

$$\begin{aligned} O_g &= \Phi^\dagger \Phi G_{\mu\nu}^a G^{\mu\nu a}, & O_t &= Y_t (\Phi^\dagger \Phi) (\bar{Q}_{3L} t_R \tilde{\Phi}), \\ O_{3g} &= f^{abc} G_{\mu\nu}^a G_{\nu\rho}^b G_{\rho\mu}^c, & O_b &= Y_b (\Phi^\dagger \Phi) (\bar{Q}_{3L} b_R \tilde{\Phi}). \end{aligned} \quad (2)$$

Here  $\Phi$  denotes the SM Higgs doublet,  $G_{\mu\nu}^a$  the QCD field strength tensor,  $Q_{3L}$  the left-handed third generation quark doublet, and  $t_R$  and  $b_R$  the right-handed top and bottom singlets, respectively. Furthermore,  $Y_t$  and  $Y_b$  are the top and bottom Yukawa couplings,  $f^{abc}$  the  $SU(3)$  structure constants and  $\tilde{\Phi} = i\sigma_2 \Phi^*$ , where  $\sigma_2$  is the second Pauli matrix. Note that  $\mathcal{L}_6$  does not represent the complete list of dimension six operators contributing to Higgs+jet observables. As stated in the introduction we are mainly interested in the contributions from  $O_{3g}$  and only include the other operators for illustrative purposes.

The main effect of  $O_t$  and  $O_b$  is to modify the  $Ht\bar{t}$  and  $Hb\bar{b}$  vertex, respectively. The corresponding coupling ratios are

$$\begin{aligned} \kappa_t &= \frac{g_{Ht\bar{t}}^{\text{SM}} + \delta g_{Ht\bar{t}}^{\text{NP}}}{g_{Ht\bar{t}}^{\text{SM}}} = 1 - \frac{v^2}{2\Lambda^2} C_t, \\ \kappa_b &= \frac{g_{Hb\bar{b}}^{\text{SM}} + \delta g_{Hb\bar{b}}^{\text{NP}}}{g_{Hb\bar{b}}^{\text{SM}}} = 1 - \frac{v^2}{2\Lambda^2} C_b, \end{aligned} \quad (3)$$

where  $v = 246$  GeV is the Higgs vacuum expectation value,  $g_{Ht\bar{t}}^{\text{SM}}$  and  $g_{Hb\bar{b}}^{\text{SM}}$  denote the SM values of the  $Ht\bar{t}$  and  $Hb\bar{b}$  couplings and  $\delta g_{Ht\bar{t}}^{\text{NP}}$  and  $\delta g_{Hb\bar{b}}^{\text{NP}}$  are the shifts in these couplings due to contributions from the operators  $O_t$  and  $O_b$ , respectively.

The operator  $O_g$  generates couplings of one or two Higgs bosons to two, three or four gluons. Normalising the  $Hgg$  coupling in the infinite top mass limit to the corresponding SM coupling leads to the coupling ratio

$$\kappa_g = \frac{g_{Hgg}^{\text{SM,eff}} + \delta g_{Hgg}^{\text{NP}}}{g_{Hgg}^{\text{SM,eff}}} = 1 + \frac{12\pi v^2}{\alpha_s \Lambda^2} C_g. \quad (4)$$

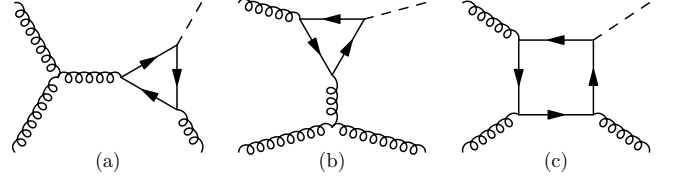


FIG. 1: Representative diagrams for  $gg \rightarrow Hg$  in the SM.

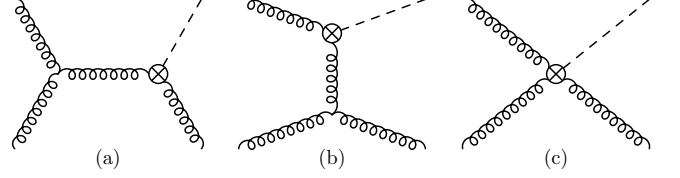


FIG. 2: Representative diagrams for  $gg \rightarrow Hg$  mediated by  $O_g$ .

Here  $g_{Hgg}^{\text{SM,eff}}$  denotes the effective SM  $Hgg$  coupling in the infinite top mass limit and  $\delta g_{Hgg}^{\text{NP}}$  the coupling induced by the operator  $O_g$ .

The operator  $O_{3g}$  generates three and four gluon vertices with a modified momentum dependence and additional vertices with up to six gluons. We do not introduce a coupling ratio for this operator.

Expected bounds on the Wilson coefficients  $C_g$ ,  $C_t$  and  $C_b$  can be derived from the bounds on  $\kappa_t$ ,  $\kappa_b$  and  $\kappa_g$  given in [19]. Using approximate limits of  $1 \pm 0.2$  on  $\kappa_t$  and  $\kappa_b$  and of  $1 \pm 0.1$  on  $\kappa_g$  as indicated by their Fig. 2 we find for  $\Lambda = 1$  TeV that

$$|C_t|, |C_b| \lesssim 6.6, \quad |C_g| \lesssim 0.0052. \quad (5)$$

Bounds on  $C_{3g}$  were estimated in [26] for a 14 TeV LHC at an integrated luminosity of  $30 \text{ fb}^{-1}$ . Translating their Fig. 7 into our conventions we find for  $\Lambda = 1$  TeV

$$|C_{3g}| \lesssim 0.12. \quad (6)$$

However, it should be noted that their estimate only accounts for statistical uncertainties. It does not include parton shower effects or other uncertainties, e.g. from parton distribution functions. The actual bound might therefore be somewhat weaker.

Let us now turn to Higgs production in association with one jet. In the SM the  $gg \rightarrow Hg$  reaction proceeds mainly through top-loop diagrams like the ones shown in Fig. 1. Interference between top and bottom loop diagrams leads to corrections of a few percent while the square of the bottom-loop contributions are negligible. If the effective operators  $O_t$  or  $O_b$  are present they simply scale the top-loop contributions and top-bottom interference by  $\kappa_t^2$  and  $\kappa_t \kappa_b$ , respectively. Due to the smallness of the top-bottom interference contribution they can not modify the shape of kinematic distributions in a noticeable way. However, the dimension six couplings generated by  $O_g$  and  $O_{3g}$  have a non-trivial momentum dependence which can lead to very different shapes in kinematic distributions.

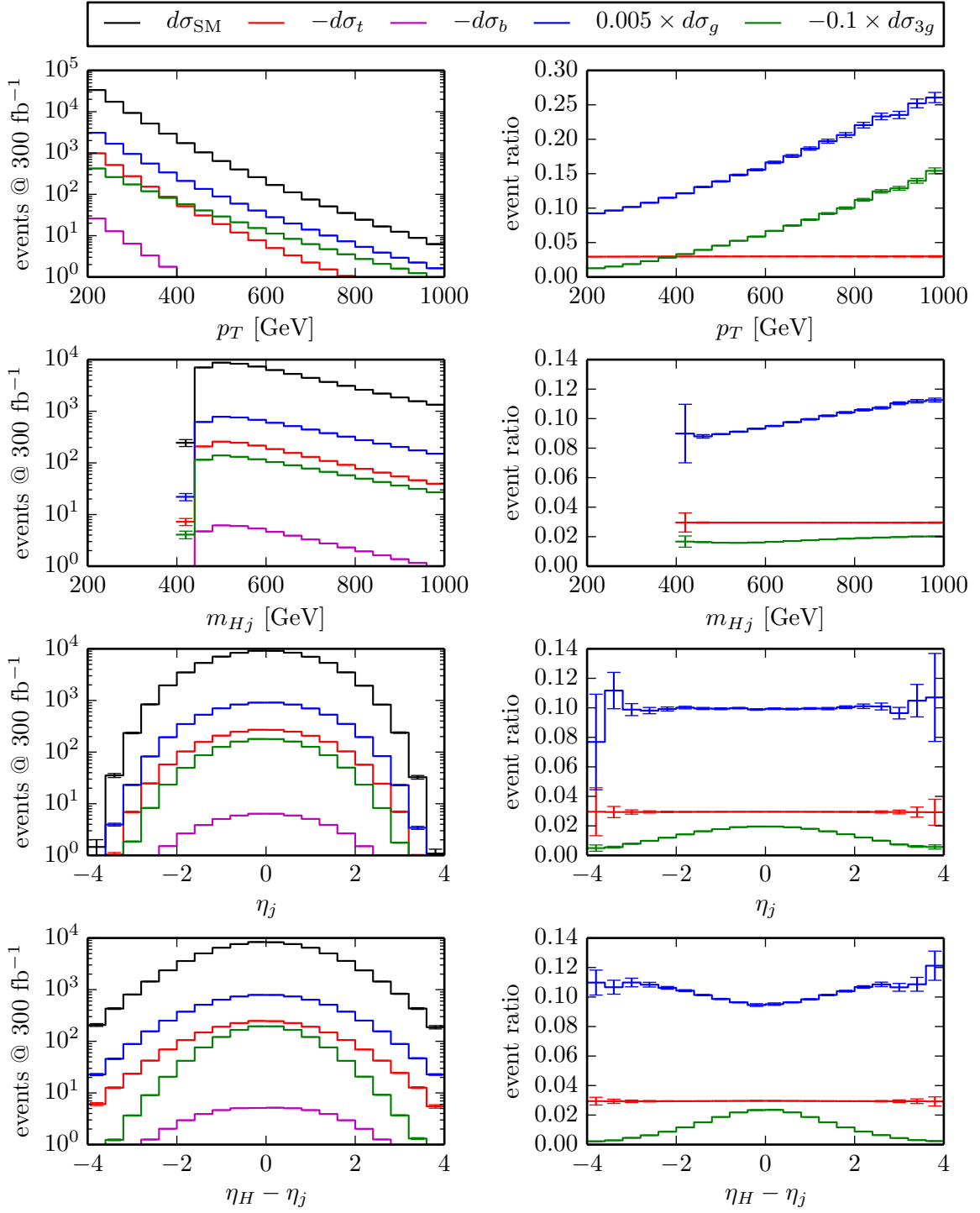


**FIG. 3:** Kinematic distributions due to the differential cross sections defined in (7) for  $\Lambda = 1$  TeV and a 14 TeV LHC. A lower  $p_T$  cut of 200 GeV was applied in all plots. Note the sign flips introduced to plot on a logarithmic scale and the scaling of  $d\sigma_g$  and  $d\sigma_{3g}$ ! The left column shows event counts for an integrated luminosity of  $300 \text{ fb}^{-1}$ . The right column shows event ratios normalised to the contribution from  $d\sigma_{\text{SM}}$ . See text for further details.

The couplings generated by  $O_g$  lead to tree-level diagrams like the ones shown in Fig. 2. As discussed in [17–19], these contributions modify the shape of the transverse momentum distribution in  $gg \rightarrow Hg$  and can be

used to discriminate between  $\kappa_t$  and  $\kappa_g$  (or equivalently  $C_t$  and  $C_g$ ). The operator  $O_{3g}$  modifies the momentum dependence of the three gluon vertex. It therefore contributes to  $gg \rightarrow Hg$  through diagrams like Fig. 1(a) and

(b). The effect of these contributions on kinematic distributions in  $gg \rightarrow Hg$  have not yet been discussed in the literature and are the main result of our analysis.

### III. KINEMATIC DISTRIBUTIONS

Let  $d\sigma$  denote the gluon fusion contribution to the differential hadronic cross section for Higgs production in association with one jet in the presence of the effective operators (2). We linearise  $d\sigma$  in the Wilson coefficients from (1) and write

$$d\sigma = d\sigma_{\text{SM}} + C_t d\sigma_t + C_b d\sigma_b + C_g d\sigma_g + C_{3g} d\sigma_{3g} \quad . \quad (7)$$

Note that, since we expand in dimensionless Wilson coefficients,  $d\sigma_t$ ,  $d\sigma_b$ ,  $d\sigma_g$ , and  $d\sigma_{3g}$  depend on the cutoff scale  $\Lambda$  and scale as  $\Lambda^{-2}$ .

We have computed the differential cross sections  $d\sigma_{\text{SM}}$ ,  $d\sigma_t$ ,  $d\sigma_b$ ,  $d\sigma_g$ , and  $d\sigma_{3g}$  using the full one-loop result for the top and bottom loops (see Fig. 1). A number of tools were used for the computation. The Feynman rules for the effective operators were generated with FeynRules 2.0 [28] and diagrams were generated with FeynArts 3.8 [29]. The analytical computations were done with the Mathematica package HEPMath [30]. The results were cross-checked with FormCalc 8.3 [31, 32] and one-loop tensor integrals were computed numerically with LoopTools 2.9 [31]. We used leading order parton distribution functions (PDFs) from CTEQ (CTEQ6L1) [33] via the LHAPDF interface. The factorisation and renormalisation scales were set to the top mass.

The left column of Fig. 3 shows histograms of the differential cross sections  $d\sigma_{\text{SM}}$ ,  $d\sigma_t$ ,  $d\sigma_b$ ,  $d\sigma_g$ , and  $d\sigma_{3g}$  for  $\Lambda = 1 \text{ TeV}$  as functions of different kinematic variables. Specifically, we show distributions of the transverse momentum  $p_T$  of the jet, the invariant mass  $m_{Hj}$  of the Higgs boson and the jet, the rapidity  $\eta_j$  of the jet and

$$\Delta\eta = \eta_H - \eta_j \quad , \quad (8)$$

where  $\eta_H$  is the rapidity of the Higgs boson. A lower  $p_T$  cut of 200 GeV was applied in all cases. For convenience the cross sections in each bin were converted to event counts assuming an integrated luminosity of  $300 \text{ fb}^{-1}$ . Note, however, that no parton shower or detector effects are included in our analysis. To better visualise the different shapes of the kinematic distributions generated by the operators  $O_g$  and  $O_{3g}$  we divided  $d\sigma_t$ ,  $d\sigma_g$ , and  $d\sigma_{3g}$  by  $d\sigma_{\text{SM}}$  and plot the ratios in the right column of Fig. 3. The error bars only contain the numerical integration error. No uncertainties due to statistics, PDFs, luminosity etc. are included. Note that  $d\sigma_t$ ,  $d\sigma_b$ ,  $d\sigma_g$  and  $d\sigma_{3g}$  are scaled with factors  $-1$ ,  $-1$ ,  $0.005$  and  $-0.1$ , respectively. The scales were chosen to be of the same order as the expected bounds on the Wilson coefficients, as discussed in Sec. II. The signs were chosen in order to be able to plot on a logarithmic scale.

From the right column of Fig. 3 we see that  $O_t$  does not modify the shape of kinematic distributions in a noticeable way. Theoretically, a small variation should be present due to the top-bottom interference contribution to  $d\sigma_{\text{SM}}$ , but this is too small to be visible in the figure. The relative size of the contribution from  $O_g$  grows larger with large  $p_T$ , in accordance with the findings of [17–19]. In addition we see that  $m_{Hj}$  and  $\Delta\eta$  are also useful for discriminating between  $O_g$  and  $O_t$ . Note that only the *shape* of the ratios shown in the right column of Fig. 3 is relevant for distinguishing the different operators. In particular, a constant offset of the ratio curve for, say,  $O_g$  can not be distinguished from a contribution from  $O_t$ .

From the top-right plot of Fig. 3 we see that the  $p_T$  distribution due to  $O_{3g}$  is a linear combination of the distributions due to  $O_g$  and  $O_t$ . Using only  $p_T$  distributions (and treating  $C_t$  as a free parameter in the fit) it is therefore not possible to distinguish between  $O_g$  and  $O_{3g}$ . This new degeneracy can be broken by considering other kinematic variables such as  $\eta_j$  and  $\Delta\eta$ . In particular, the ratio curve for  $O_g$  in the variable  $\eta_j$  is completely flat while the one for  $O_{3g}$  is peaked around  $\eta_j = 0$ . Disregarding constant offsets the variations of the ratio curves for  $O_{3g}$  are of the same size as the variations for  $O_g$  if the Wilson coefficients of both operators are of the order of the expected bounds. Thus the possible impact of  $O_{3g}$  on Higgs+jet observables is as large as that of  $O_g$ .

### IV. CONCLUSIONS

Higgs production in association with a jet receives contributions not only from effective dimension six operators involving the Higgs doublet but also from the triple gluon operator  $O_{3g}$ . In this paper we have calculated the differential cross section for  $gg \rightarrow Hg$  in the presence of the dimension six operators  $O_{3g}$ ,  $O_g$ ,  $O_t$  and  $O_b$ . To the best of our knowledge the contributions due to  $O_{3g}$  have not yet been discussed in the literature. We find that the distributions of the transverse momentum  $p_T$  of the jet are insufficient to discriminate between  $O_g$  and  $O_{3g}$  if the Wilson coefficient of  $O_t$  is free to float in the fit. This new degeneracy can be broken by considering distributions in the jet rapidity  $\eta_j$  and the difference  $\Delta\eta$  between the Higgs and jet rapidity. In particular, the shape of the  $\eta_j$  distribution is only modified by  $O_{3g}$  but not by  $O_g$  or  $O_t$ . The distortions due to  $O_{3g}$  are of the same size as the distortions due to  $O_g$  if the Wilson coefficients of both operators are of the order of the expected bounds. Consequently, a full model independent analysis of new physics in Higgs+jet observables must take the contributions from  $O_{3g}$  into account.

#### Acknowledgements

This work is supported by the European Research Council under the European Union's Seventh Framework

Programme (FP/2007-2013) / ERC Grant Agreement n.279972. DG thanks Michael Spannowsky for hospital-

ity in the IPPP, Durham University where this project was envisaged, and Roberto Contino for discussions.

- 
- [1] B. Grzadkowski, M. Iskrzynski, M. Misiak, and J. Rosiek, *JHEP* **1010**, 085 (2010), [arXiv:1008.4884 \[hep-ph\]](#).
  - [2] R. Contino, M. Ghezzi, C. Grojean, M. Mühlleitner, and M. Spira, *JHEP* **1307**, 035 (2013), [arXiv:1303.3876 \[hep-ph\]](#).
  - [3] E. E. Jenkins, A. V. Manohar, and M. Trott, *JHEP* **1310**, 087 (2013), [arXiv:1308.2627 \[hep-ph\]](#).
  - [4] E. E. Jenkins, A. V. Manohar, and M. Trott, *JHEP* **1401**, 035 (2014), [arXiv:1310.4838 \[hep-ph\]](#).
  - [5] T. Corbett, O. Eboli, J. Gonzalez-Fraile, and M. Gonzalez-Garcia, *Phys.Rev.* **D87**, 015022 (2013), [arXiv:1211.4580 \[hep-ph\]](#).
  - [6] B. Dumont, S. Fichet, and G. von Gersdorff, *JHEP* **1307**, 065 (2013), [arXiv:1304.3369 \[hep-ph\]](#).
  - [7] J. Elias-Miro, J. Espinosa, E. Masso, and A. Pomarol, *JHEP* **1311**, 066 (2013), [arXiv:1308.1879 \[hep-ph\]](#).
  - [8] A. Pomarol and F. Riva, *JHEP* **1401**, 151 (2014), [arXiv:1308.2803 \[hep-ph\]](#).
  - [9] L. G. Almeida, S. J. Lee, S. Pokorski, and J. D. Wells, *Phys.Rev.* **D89**, 033006 (2014), [arXiv:1311.6721 \[hep-ph\]](#).
  - [10] R. Alonso, E. E. Jenkins, A. V. Manohar, and M. Trott, *JHEP* **1404**, 159 (2014), [arXiv:1312.2014 \[hep-ph\]](#).
  - [11] J. Ellis, V. Sanz, and T. You, *JHEP* **1407**, 036 (2014), [arXiv:1404.3667 \[hep-ph\]](#).
  - [12] J. de Blas, M. Ciuchini, E. Franco, D. Ghosh, S. Mishima, *et al.*, (2014), [arXiv:1410.4204 \[hep-ph\]](#).
  - [13] J. Ellis, V. Sanz, and T. You, (2014), [arXiv:1410.7703 \[hep-ph\]](#).
  - [14] ATLAS conference note, ATLAS-CONF-2014-009 ().
  - [15] CMS physics analysis summary, CMS-PAS-HIG-14-009.
  - [16] R. V. Harlander and T. Neumann, *Phys.Rev.* **D88**, 074015 (2013), [arXiv:1308.2225 \[hep-ph\]](#).
  - [17] A. Banfi, A. Martin, and V. Sanz, *JHEP* **1408**, 053 (2014), [arXiv:1308.4771 \[hep-ph\]](#).
  - [18] A. Azatov and A. Paul, *JHEP* **1401**, 014 (2014), [arXiv:1309.5273 \[hep-ph\]](#).
  - [19] C. Grojean, E. Salvioni, M. Schlaffer, and A. Weiler, *JHEP* **1405**, 022 (2014), [arXiv:1312.3317 \[hep-ph\]](#).
  - [20] M. Schlaffer, M. Spannowsky, M. Takeuchi, A. Weiler, and C. Wymant, *Eur.Phys.J.* **C74**, 3120 (2014), [arXiv:1405.4295 \[hep-ph\]](#).
  - [21] J. S. Gainer, J. Lykken, K. T. Matchev, S. Mrenna, and M. Park, (2014), [arXiv:1403.4951 \[hep-ph\]](#).
  - [22] M. Buschmann, C. Englert, D. Goncalves, T. Plehn, and M. Spannowsky, *Phys.Rev.* **D90**, 013010 (2014), [arXiv:1405.7651 \[hep-ph\]](#).
  - [23] M. Buschmann, D. Goncalves, S. Kuttimalai, M. Schonherr, F. Krauss, *et al.*, (2014), [arXiv:1410.5806 \[hep-ph\]](#).
  - [24] C. Englert and M. Spannowsky, (2014), [arXiv:1408.5147 \[hep-ph\]](#).
  - [25] S. Dawson, I. Lewis, and M. Zeng, (2014), [arXiv:1409.6299 \[hep-ph\]](#).
  - [26] P. L. Cho and E. H. Simmons, *Phys.Rev.* **D51**, 2360 (1995), [arXiv:hep-ph/9408206 \[hep-ph\]](#).
  - [27] ATLAS conference note, ATLAS-CONF-2014-057 ().
  - [28] A. Alloul, N. D. Christensen, C. Degrande, C. Duhr, and B. Fuks, *Comput.Phys.Commun.* **185**, 2250 (2014), [arXiv:1310.1921 \[hep-ph\]](#).
  - [29] T. Hahn, *Comput.Phys.Commun.* **140**, 418 (2001), [arXiv:hep-ph/0012260 \[hep-ph\]](#).
  - [30] M. Wiebusch, (2014), [arXiv:1412.6102 \[hep-ph\]](#).
  - [31] T. Hahn and M. Perez-Victoria, *Comput.Phys.Commun.* **118**, 153 (1999), [arXiv:hep-ph/9807565 \[hep-ph\]](#).
  - [32] T. Hahn, *Comput.Phys.Commun.* **178**, 217 (2008), [arXiv:hep-ph/0611273 \[hep-ph\]](#).
  - [33] J. Pumplin, D. Stump, J. Huston, H. Lai, P. M. Nadolsky, *et al.*, *JHEP* **0207**, 012 (2002), [arXiv:hep-ph/0201195 \[hep-ph\]](#).